Journal of Global Change Data & Discovery. 2022, 6(3): 330-338
www.geodoi.ac.cn

Establishment of a Yearly September–October Mean Temperature Dataset during 1678–2019 in Northwest Yunnan Province, China

Deng, G. F.[1,2] Li, M. Q.[1*]

1. Key Laboratory of Land Pattern and Simulation, Institute of Geographic Science and Natural Resources Research, Chinese Academy of Sciences, Beijing 100101, China;
2. University of Chinese Academy of Sciences, Beijing 100049, China

Abstract: Tree-ring cores were collected from *Abies delavayi* Franch. in November 2012 and 2019. The sampling site was in Gongshan Dulong and Nu autonomous county, Yunnan province (98.48°E, 27.78°N; 3,245 m a.s.l.). X-ray imaging was employed to obtain density data. Then, the program ARSTAN was used to detrend and normalize the data, in which a 67% cubic smoothing spline with a 50% cut-off frequency was employed to fit the growth trend. Ultimately, we retained the maximum latewood density (MXD) of 51 cores from 27 trees for establishing a chronology of the period 1678–2019. Based on the correlations between MXD and climate variables, the residual chronology of MXD showed its strongest correlation with the September–October mean temperature ($T_{9–10}$). Thus, a transfer function was established with a linear regression model to reconstruct the $T_{9–10}$ during the past 342 years (1678–2019), with an explained variance of 33% during the instrumental period. Leave-one-out cross-validation showed the robustness of the reconstruction, with a reduction of error reaching 0.29. Furthermore, the temperature series correlated positively with other reconstructions in the surrounding areas, with correlation coefficients of 0.458–0.526. The dataset includes: (1) geographical information of the sampling site; (2) the statistical characteristics of tree-ring cores; (3) the residual chronology of the MXD for *A. delavayi* and its reconstructed series of $T_{9–10}$; (4) the tree-ring residual chronology statistics of the MXD for *A. delavayi*; and (5) the temperature data used for the reconstruction. The dataset is archived in .shp and .xlsx data formats, and consists of seven data files with a total data size of 56.5 KB (compressed to a single 52.5 KB file).

Keywords: northwestern Yunnan province; maximum latewood density; temperature reconstruction; long chronology

DOI: https://doi.org/10.3974/geodp.2022.03.02

CSTR: https://cstr.escience.org.cn/CSTR:20146.14.2022.03.02

Received: 20-04-2022; **Accepted:** 11-07-2022; **Published:** 25-09-2022

Foundations: National Natural Science Foundation of China (41977391, 41630529, 41571194); Ministry of Science and Technology of P. R. China (2017YFA0603302)

***Corresponding Author:** Li, M. Q., Institute of Geographic Science and Natural Resources Research, Chinese Academy of Sciences, limq@igsnrr.ac.cn

Data Citation: [1] Deng, G. F., Li, M. Q. Establishment of a yearly September–October mean temperature dataset during 1678–2019 in northwest Yunnan province, China [J]. *Journal of Global Change Data & Discovery*, 2022, 6(3): 330–338. https://doi.org/10.3974/geodp.2022.03.02. https://cstr.escience.org.cn/CSTR:20146.14.2022.03.02.

[2] Deng, G. F., Li, M. Q. Reconstruction dataset of yearly September–October mean temperature from tree-ring maximum latewood density of *Abies delavayi* Franch. at northwest Yunnan province of China (1678–2019) [J/DB/OL]. *Digital Journal of Global Change Data Repository*, 2022. https://doi.org/10.3974/geodb.2022.04.03.V1. https://cstr.escience.org.cn/CSTR:20146.11.2022.04.03.V1.

Dataset Availability Statement:

The dataset supporting this paper was published and is accessible through the *Digital Journal of Global Change Data Repository* at: https://doi.org/10.3974/geodb. 2022.04.03.V1 or https://cstr.escience.org.cn/CSTR:20146.11.2022.04.03.V1.

1 Introduction

Tree rings are widely used to reconstruct historical climate change because of their broad distribution, high resolution, and accurate dating, providing fundamental materials for exploring the driving mechanisms of climate change. Situated southeast of the Tibetan Plateau (TP) and north of the Hengduan Mountains, the terrain of northwestern Yunnan province is characterized by deep valleys with steep sides, resulting in large horizontal and vertical differences in climate. These complex geographical conditions have resulted in a diverse range of tree species in our study area, such as *Larix speciosa* Cheng et Law, *Abies delavayi* Franch., and *Tsuga dumosa* (D. Don) Eichler[1,2]. Such an abundance and richness of tree species help to provide sufficient tree-ring materials for climate reconstruction. Owing to the warm and humid climate in northwestern Yunnan province, the latewood density of conifers in high-altitude areas is mainly affected by temperature in the growing season. Previous studies have used the maximum latewood density (MXD) from *L. speciosa*, *Picea asperata* Mast., and *Picea brachytyla* (Franch.) Pritz. var. *complanata* (Mast.) Cheng ex Rehd. to reconstruct the mean temperature of the growing season or late summer in the study area[3–5], and the longest of which is a 319-year reconstruction of the August–September mean temperature based on the MXD of *L. speciosa*. However, previous MXD-based reconstructions show inconsistent warming trends over the past 30 years in the eastern TP.

Analyses reveal that the climate in eastern Tibetan autonomous region and western Sichuan has warmed faster than in northwestern Yunnan province[6,7]. Such inconsistency may be attributable to the detrending methods used or the environmental differences among sampling sites across different studies[6,8]. The MXD used for reconstructions primally derives from *P. likiangensis* var. *balfouriana* in eastern Tibetan autonomous region and western Sichuan province, along with *L. speciosa*, *A. georgei Orr* var. *smithii* (Viguie et Gaussen) Cheng et L., and *P. asperata* in northwestern Yunnan province. Studies suggest that MXD-based reconstructions from different species have different explained variances[4,5,7,9–14]. Therefore, more MXD-based reconstructions from different tree species should be carried out to explore the possible influence of genetic factors. In this study, a September–October temperature dataset for the period 1678–2019 in northwestern Yunnan was reconstructed based on the MXD of *A. delavayi*, which is longer than previous MXD-based proxy records. This series provides a useful reference for exploring the potential of tree-ring density from different species in climate reconstruction.

2 Metadata of the Dataset

The details of the September–October mean temperature dataset[15] during 1678–2019 in northwestern Yunnan are shown in Table 1, including the dataset's full name, short name, its authors, coverage period, temporal resolution, data format, data size, data files, data publisher, and data sharing policy, etc.

3 Methods

3.1 Algorithm

Pearson's correlation coefficients between the MXD chronology and mean monthly temperature and monthly precipitation during 1951–2019 were calculated. The results indicated that the mean temperature of September–October ($T_{9–10}$) has the highest correlation with MXD. Linear regression was then performed to establish the transfer

function using MXD as predictors. After calibration, we introduced the correlation coefficient between the reconstructed value and the observed value (*r*), sign test (*ST, ST1*), product mean test (*T*), reduction error (*RE*) and validity coefficient (*CE*) for verification[17].

Table 1 Metadata summary of the Reconstruction dataset of yearly September-October mean temperature from tree-ring maximum latewood density of *Abies delavayi Franch*. at northwest Yunnan province of China (1678–2019)

Items	Description
Dataset full name	Reconstruction dataset of yearly September-October mean temperature from tree-ring maximum latewood density of *Abies delavayi Franch*. at northwest Yunnan province of China (1678–2019)
Dataset short name	MeanTemp9-10nwYunnan1678-2019
Authors	Deng, G. F., Institute of Geographic Science and Natural Resources Research, Chinese Academy of Sciences, dengguofu18@mails.ucas.ac.cn Li, M. Q., Institute of Geographic Science and Natural Resources Research, Chinese Academy of Sciences, limq@igsnrr.ac.cn
Geographical region	Northwestern Yunnan province, China
Coverage	342 years (1678–2019)
Temporal resolution	Yearly
Data format	.shp, .xlsx
Data size	56.5 KB (52.5 KB after compressed)
Data files	(1) Geographical information of sampling site; (2) statistical characteristics of tree-ring cores; (3) residual chronology of the MXD of *A. delavayi* and its reconstructed series of $T_{9–10}$; (4) tree-ring residual chronology statistics of the MXD of *A. delavayi*; and (5) temperature data used for reconstruction
Foundations	National Natural Science Foundation of China (41977391, 41630529, 41571194); Ministry of Science and Technology of P. R. China (2017YFA0603302)
Data publisher	Global Change Research Data Publishing & Repository, http://www.geodoi.ac.cn
Address	No. 11A, Datun Road, Chaoyang District, Beijing 100101, China
Data sharing policy	***Data*** from the Global Change Research Data Publishing & Repository includes metadata, datasets (in the *Digital Journal of Global Change Data Repository*), and publications (in the *Journal of Global Change Data & Discovery*). ***Data*** sharing policy includes: (1) ***Data*** are openly available and can be free downloaded via the Internet; (2) End users are encouraged to use ***Data*** subject to citation; (3) Users, who are by definition also value-added service providers, are welcome to redistribute ***Data*** subject to written permission from the GCdataPR Editorial Office and the issuance of a ***Data*** redistribution license; and (4) If ***Data*** are used to compile new datasets, the 'ten per cent principal' should be followed such that ***Data*** records utilized should not surpass 10% of the new dataset contents, while sources should be clearly noted in suitable places in the new dataset[16]
Communication and searchable system	DOI, CSTR, Crossref, DCI, CSCD, CNKI, SciEngine, WDS/ISC, GEOSS

The calculation of the test statistic T of the product mean test is as follows:

$$T = \frac{\left(M_1 - M_2\right)}{\sqrt{\frac{S_1^2}{N_1} + \frac{S_2^2}{N_2}}} \tag{1}$$

If the sign of the calibration anomaly is the same as the observed data anomaly, the product of two anomalies is divided into positive groups. Otherwise, the product is added to the negative group. M_1 and M_2 are the means of all positive and negative products, respectively. S_1^2 an N_1 are the variance and number of products of the positive product group, while S_2^2 and N_2 are the corresponding values of the negative product group.

The *RE* and *CE* are computed as:

$$RE = 1 - \frac{\sum\left(y_i - \hat{y}_i\right)^2}{\sum\left(y_i - \overline{y}_c\right)^2} \tag{2}$$

$$CE = 1 - \frac{\sum (y_i - \hat{y}_i)^2}{\sum (y_i - \overline{y}_v)^2} \tag{3}$$

The variables y_i and $\hat{y}_i$ are the observed and reconstructed values during the verification periods. The variables $\overline{y}_c$ and $\overline{y}_v$ are the observed mean during the calibration and verification period, respectively. When both *RE* and *CE* are above zero, a high reliability of the reconstruction is suggested.

3.2 Data Collection and Processing

Tree-ring increment cores were collected in November 2012 and 2019 at a mixed forest of *L. speciosa* and *A. delavayi*. The sampling site was on a southwest-facing mountain slope at 98.48°E, 27.78°N (3,245 m a.s.l.) in the north of the Gaoligong Mountains (Figure 1). To begin with, the tree-ring cores were kept under natural conditions for drying, and were cross-dated by a microscope. Then, the tree-ring width was measured using the LINTAB6 measurement system with 0.01-mm precision. Next, the processes of splitting and supporting, measuring fiber angles, cutting to slices, eliminating resins, taking X-ray photography, developing films, and measuring density were carried out. After obtaining MXD raw measurements, the program ARSTAN was employed to develop MXD chronologies, with a 67% cubic smoothing spline to fit the growth trend of each series[18]. Based on the residual chronology of the MXD and gridded temperature data from CRU TS4.04 (average data of 98.25°E, 27.75°N and 98.75°E, 27.75°N)[1], linear regression analysis was performed to establish the transfer function between $T_{9–10}$ and MXD during 1951–2019. This function was then used to reconstruct $T_{9–10}$ for the historical period, and the series was compared with other reconstructions in the eastern TP (Figure 2).

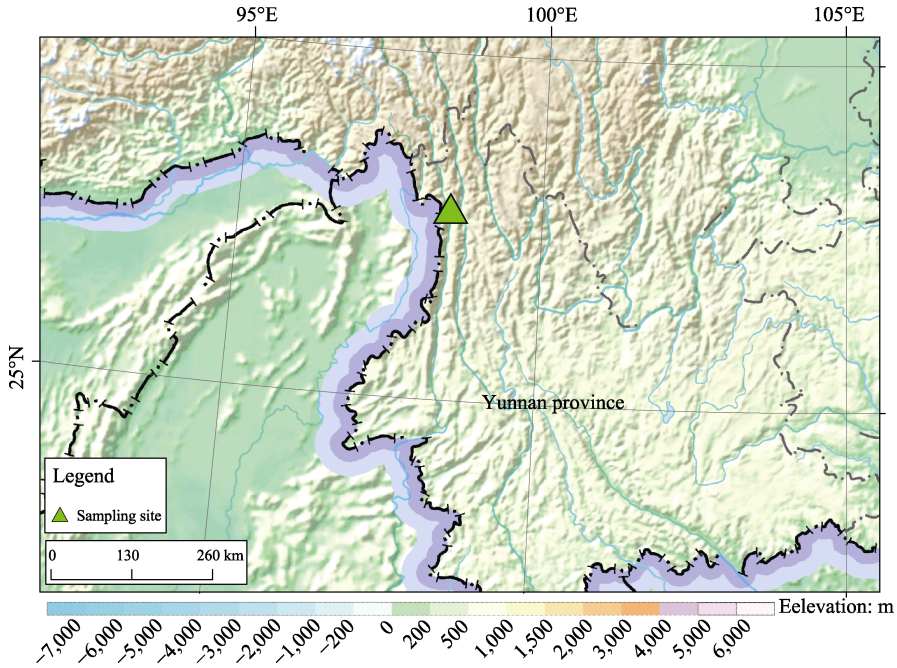

Figure 1 Location of the sampling site

[1] https://catalogue. ceda.ac.uk/.

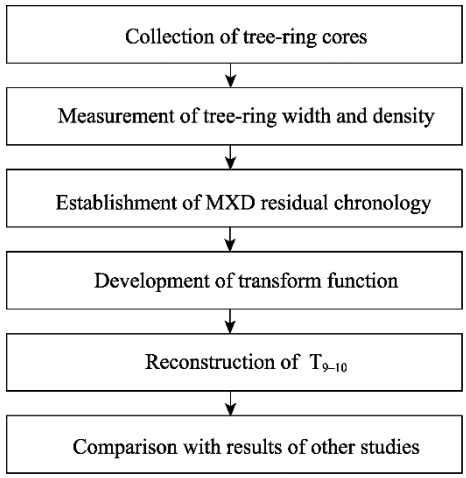

Figure 2 Flowchart showing the process of $T_{9–10}$ reconstruction in northwest Yunnan province

4 Data Results and Validation

4.1 Data Composition

The dataset includes (1) geographical information of the sampling site; (2) statistical characteristics of tree-ring cores; (3) the residual chronology of the MXD of *A. delavayi* and its reconstructed series of $T_{9–10}$; (4) tree-ring residual chronology statistics for the MXD of *A. delavayi*, and (5) the temperature data used for reconstruction. The dataset is archived in .shp and .xlsx data formats, and consists of 7 data files with a total data size of 56.5 KB (Compressed to a single 52.5 KB file).

4.2 Data Results

The reconstruction of $T_{9–10}$ covered the period 1678–2019 A.D. (Figure 3). The regression produced the following linear model for the calibration period of 1951–2019: $T_{9–10} = 10.43 \times MXD + 8.37$. The model explained 33% ($R_{adj}^2 = 32\%$) of the variance for the instrumental period. The statistics of the calibration and validation are given in Table 2. The sign test results of the leave-one-out cross validation are statistically significant at the 0.05 level. The values of *RE* and the product mean t also passed the tests, suggesting good estimation skill, with a correlation of 0.54 between observed values and calibrated ones. We also performed a split-period validation. For the calibration period of 1951–1985, the sign tests for the first-difference data (*ST1*) reached the 95% confidence level. Moreover, the *RE* and *CE* values were above zero, suggesting good agreement between the predicted and observed values. For the calibration period of 1986–2019, the sign tests for the original value did not reach the 95% confidence level, and the *CE* was lower than zero. Although some test results were not statistically significant during the calibration period of 1986–2019, the test results were statistically significant for the calibration periods of 1951–2019 and 1951–1985. The validation results suggest that the model is relatively robust, with sufficient estimation skill.

Based on an 11-year moving average of the reconstruction, warm intervals higher than the average historical temperature occurred in 1683–1688, 1719–1731, 1746–1776, 1788–1808, 1862–1879, 1904–1921, 1949–1978, and 2003–2014. Conversely, a cold autumn appeared in 1689–1701, 1707–1718, 1738–1745, 1777–1782, 1809–1826, 1828–1846, 1885–1890, 1922–1944, and 1981–2002. The coldest period of the past 342 years was 1809–1826, with a September–October mean temperature of 18.7 °C, and the warmest one was in 1788–1808, with a mean temperature of 18.9 °C. Furthermore, the dataset shows the warmest autumn

Table 2 Statistics of calibration and validation

Calibration					Validation						
Period	R^2	Radj^2	F	SE	Period	*r*	*ST*	*ST1*	t	*RE*	*CE*
1951–2019	33	32	33.05	0.48	1951–2019	0.54	53+/16*	56+/11*	2.62	0.29	
1951–1985	29.7	27.6	13.95	0.48	1986–2019	0.68	23+/11–	27+/6–*	2.10	0.29	0.18
1986–2019	46.5	44.8	27.76	0.44	1951–1985	0.55	23+/12–	28+/6**	2.50	0.08	–0.06

Notes: R^2, explained variance; Radj^2, adjusted explained variance; F, the F statistic for the statistical significance of the linear models; SE, standard error; *r*, the correlation between observed values and reconstructed ones during the verification period; *ST*, sign test; *ST1*, sign test of first difference; t, the *T* statistic for the product mean test; *RE*, reduction of error; *CE*, coefficient of efficiency; * 95% confidence level; ** 99% confidence level.

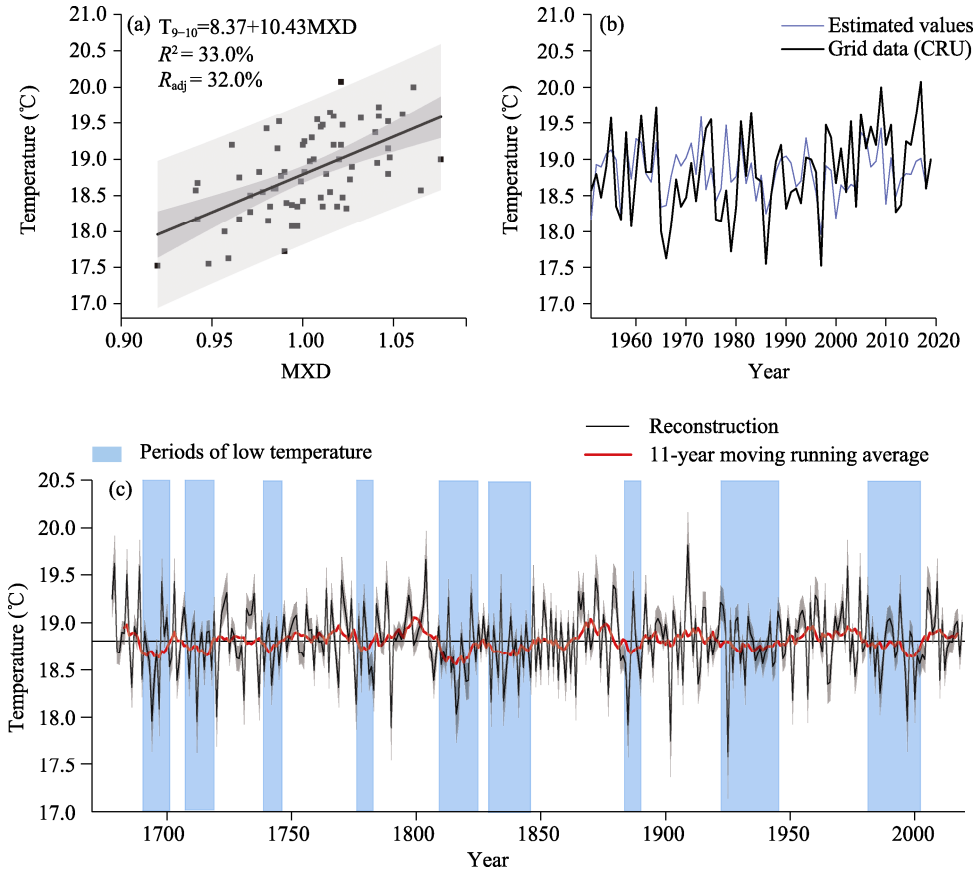

Figure 3 Scatter plot (a) and graph (b) of the gridded and estimated September–October mean temperature ($T_{9–10}$) for the calibration period of 1951–2019. (c) Reconstructed September–October mean temperature (thin line) and 11-year smoothing (thick line) from Gongshan, northwestern Yunnan province, based on the MXD during 1678–2019. The gray area denotes the 95% confidence interval. The vertical shading indicated the periods of low temperature in the reconstructed $T_{9–10}$ series when the 11-year smoothed values were lower than the long-term mean

has occurred in 1909, while the coldest year was in 1925, with differences of 2.2 °C between the early-autumn temperature of these two years.

4.3 Comparisons with Other Temperature Reconstructions in the Eastern TP

To further assess the reliability of our reconstructed series, we also compared it with other MXD-based temperature reconstructions in the eastern TP. The target season and the

distance to our sampling site for other reconstructions may cause discriminations during some periods. Additionally, the shorter the distance to our sampling site and the closer to September–October, the higher the correlation between other reconstructions and our results.

For example, the MXD-based temperature series from the Yulong Mountain and the Gaoligong Mountains had correlation coefficients of 0.526 (p<0.001, 1707–2010) and 0.509 (p<0.001, 1707–2008) with our results, respectively[3,5]. The temperature series for the sampling site near Leiwuqi correlated to our reconstruction with a coefficient of 0.458 (p<0.001, 1765–2009), while the August–September mean temperature series from Sygera Mountain and the April–September mean temperature from the Central Hengduan mountains had lower correlations of 0.282 (p<0.001, 1820–2008) and 0.237 (p<0.001, 1707–2006) with our reconstructed series, respectively. Furthermore, according to the low-frequency variation of these results, similar temperature variations occurred in many periods for *L. speciosa*, *A. delavayi*, and *P. asperata*. It was relatively warm in 1795–1805, 1865–1880 and 1940–1960, while it was relatively cold in 1810–1820, 1850–1860, 1935–1942 and 1990–2004. Thus, the correlation and the common low-frequency variations testify the reliability of our dataset.

MXD-based reconstructions from different species have differences in their low-frequency variations. Series from *L. speciosa*, *A. delavayi* and *P. asperata* showed different trends during 1750–1770, 1820–1850 and 1900–1920, despite their sampling sites being close to our study. The temperature increased in 1750–1770 and 1900–1920 according to the MXD-based reconstruction from *L. speciosa* and *P. brachytyla*, but not from *P. asperata*. The proxy records from *A. georgei* showed contrary variations to our series in 1860–1880 and 1930–1970. In addition, *P. likiangensis* also presented different trends to our reconstruction in 1900–1950. Moreover, the series from *P. asperata*, *P. brachytyla*, *P. likiangensis* and *A. georgei* have steeper warming rates than those from *L. speciosa* and *A. delavayi* in the latest 30 years (Figure 4).

5 Discussion and Conclusion

A September–October mean temperature dataset in northwestern Yunnan province was developed based on the MXD of *A. delavayi*. The dataset is longer than previous MXD-based series reconstructions. Our reconstruction provides a useful reference for studying historical climate change based on tree-ring width, ice cores, historical documents, and other proxy data. The dataset shows nine cold intervals and eight warm periods. It also indicates that the coldest autumn of the past 342 years occurred in 1809–1826, and the warmest period appeared in 1788–1808.

The reconstructed dataset displays high accordance with MXD-based reconstructed late-summer temperature data in northwestern Yunnan province and eastern Tibetan autonomous region, with correlation coefficients of 0.458–0.526. Moreover, the differences between this dataset and previously developed series from the central Hengduan Mountains and Sygera Mountain may stem from their different target seasons and density index. In addition, this newly reconstructed series based on the MXD of *A. georgei* expands the source of tree species for reconstruction work, and provides a reference for future studies seeking to compare the differences among reconstructions based on different tree species.

Author Contributions

Li, M. Q. designed the algorithms of the dataset. Deng, G. F. contributed to the data processing and analysis. Deng, G. F. wrote the paper.

Acknowledgements

We would like to thank Professor Zhang, Qibin, Fan, Zexin, and Dr. Li, Mingyong for providing their data for comparison.

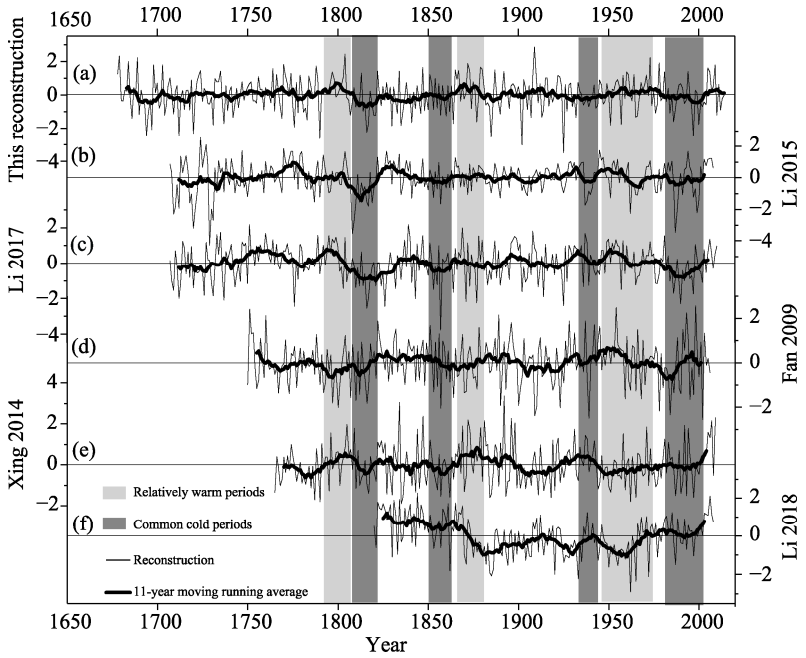

Figure 4 Comparisons of the September–October mean temperature dataset in this study (a) with other MXD-based temperature reconstructions (b–f) in the eastern TP: (b) August–September mean temperature reconstructed using MXD series from *L. speciosa* in the Gaoligong Mountains[5]; (c) July–October maximum temperature reconstructed series from Yulong Mountain, northwest Yunnan province, based on both MXD and tree-ring width of *P. asperata* [3]; (d) April–September mean temperature reconstruction from MXD series of *P. brachytyla* in the central Hengduan Mountains[4]; (e) August–September mean temperature reconstruction based on the MXD of *P. likiangensis* near to Leiwuqi in eastern Tibet[11]; (f) August–September mean temperature reconstructed series based on the mean latewood density of *A. georgei* at Sygera Mountain, southeastern Tibet. The light grey shading indicated the relatively warm periods, while the dark grey shading indicated the common cold periods

Conflicts of Interest

The authors declare no conflicts of interest.

References

[1] Ou, G. L., Xu, C. D., He, Z. R., *et al*. Quantitative classification of plant communities on the northern part of Gaoligong Mountains by TWINSPAN [J]. *Acta Botanica Yunnanica*, 2008, 30(6): 679–687.

[2] Xu, C. D., Feng, J. M., Wang, X. P., *et al*. Vertical distribution patterns of plant species diversity in northern Mt. Gaoligong, Yunnan province [J]. *Chinese Journal of Ecology*, 2008, 27(3): 323–327.

[3] Li M. Q., Huang L., Yin Z. Y., *et al.* Temperature reconstruction and volcanic eruption signal from tree-ring width and maximum latewood density over the past 304 years in the southeastern Tibetan Plateau [J]. *International Journal of Biometeorology*, 2017, 61(11): 2021–2032.

[4] Fan, Z. X., Braunin,g A., Yang, B., *et al.* Tree ring density-based summer temperature reconstruction for the

central Hengduan Mountains in southern China [J]. *Global and Planetary Change*, 2009, 65(1/2): 1–11.

[5] Li, M. Y., Wang, L., Fan, Z. X., *et al.* Tree-ring density inferred late summer temperature variability over the past three centuries in the Gaoligong Mountains, southeastern Tibetan Plateau [J]. *Palaeogeography Palaeoclimatology Palaeoecology*, 2015, 422: 57–64.

[6] Yin, H., Li, M. Y., Huang, L. Summer mean temperature reconstruction based on tree-ring density over the past 440 years on the eastern Tibetan Plateau [J]. *Quaternary International*, 2021, 571: 81–88.

[7] Duan, J. P., Ma, Z. G., Li, L., *et al.* August–September temperature variability on the Tibetan Plateau: past, present and future [J]. *Journal of Geophysical Research*: *Atmospheres*, 2019, 124(12): 6057–6068.

[8] Martinez-Sancho E., Slamova L., Morganti S., *et al.* The gen tree dendroecological collection, tree-ring and wood density data from seven tree species across Europe [J]. *Scientific Data*, 2020, 7(1): 1–17.

[9] Wang, L., Duan, J. P., Chen, J., *et al.* Temperature reconstruction from tree-ring maximum density of Balfour spruce in eastern Tibet, China [J]. *International Journal of Climatology*, 2010, 30(7): 972–979.

[10] Duan, J. P., Zhang, Q. B. A 449 year warm season temperature reconstruction in the southeastern Tibetan Plateau and its relation to solar activity [J]. *Journal of Geophysical Research*: *Atmospheres*, 2014, 119(20): 11578–11592.

[11] Xing, P., Zhang, Q. B., Lv, L. X. Absence of late-summer warming trend over the past two and half centuries on the eastern Tibetan Plateau [J]. *Global and Planetary Change*, 2014, 123: 27–35.

[12] Yin, H., Liu, H. B., Linderholm, H. W., *et al.* Tree ring density-based warm-season temperature reconstruction since A.D. 1610 in the eastern Tibetan Plateau [J]. *Palaeogeography Palaeoclimatology Palaeoecology*, 2015, 426: 112–120.

[13] Liang, H. X., Lyu, L. X., Wahab, M. A 382-year reconstruction of August mean minimum temperature from tree-ring maximum latewood density on the southeastern Tibetan Plateau, China [J]. *Dendrochronologia*, 2016, 37: 1–8.

[14] Li, M. Y., Duan, J. P., Wang, L., *et al.* Late summer temperature reconstruction based on tree-ring density for Sygera Mountain, southeastern Tibetan Plateau [J]. *Global and Planetary Change*, 2018, 163: 10–17.

[15] Deng, G. F., Li, M. Q. Reconstruction dataset of yearly September–October mean temperature from tree-ring maximum latewood density of *Abies delavayi* Franch. at northwest Yunnan province of China (1678–2019) [J/DB/OL]. *Digital Journal of Global Change Data Repository*, 2022. https://doi.org/10.3974/geodb.2022.04.03.V1. https://cstr.escience.org.cn/CSTR:20146.11.2022.04.03.V1.

[16] GCdataPR Editorial Office. GCdataPR data sharing policy [OL]. https://doi.org/10.3974/dp.policy.2014.05 (Updated 2017).

[17] Cook, E. R., Briffa, K. R., Jones, P. D. Spatial regression methods in dendroclimatology: a review and comparison of two techniques [J]. *International Journal of Climatology*, 1994, 14(4): 379–402.

[18] Cook, E. R., Kairiukstis, L. A. Methods of Dendrochronology [M]. Dordrecht, Netherlands: Springer Netherlands, 1990.